Journal of Macromolecular Science, Part A
Publication details, including instructions for authors and subscription information:
http://www.informaworld.com/smpp/title~content=t713597274

Functionalization by Cold Plasmas of Polymer Model Surfaces (Hexatriacontane and Octadecyloctadecanoate) Studied by Contact Angle Measurements, XPS, and FTIR Spectroscopy

M. K. Shi[a]; J. Christoud[a]; Y. Holl[a]; F. Clouet[a]
[a] Institut Charles Sadron (CRM-EAHP) Centre National de la Recherche Scientifique et Université, Strasbourg, Cedex, France

To cite this Article Shi, M. K. , Christoud, J. , Holl, Y. and Clouet, F.(1993) 'Functionalization by Cold Plasmas of Polymer Model Surfaces (Hexatriacontane and Octadecyloctadecanoate) Studied by Contact Angle Measurements, XPS, and FTIR Spectroscopy', Journal of Macromolecular Science, Part A, 30: 2, 219 — 239
To link to this Article: DOI: 10.1080/10601329308009401
URL: http://dx.doi.org/10.1080/10601329308009401

J.M.S.—PURE APPL. CHEM., A30(2 & 3), pp. 219–239 (1993)

FUNCTIONALIZATION BY COLD PLASMAS OF POLYMER MODEL SURFACES (HEXATRIACONTANE AND OCTADECYLOCTADECANOATE) STUDIED BY CONTACT ANGLE MEASUREMENTS, XPS, AND FTIR SPECTROSCOPY

M. K. SHI, J. CHRISTOUD, Y. HOLL, AND F. CLOUET*

Institut Charles Sadron (CRM-EAHP)
Centre National de la Recherche Scientifique et Université Louis Pasteur
6, rue Boussingault, 67083 Strasbourg Cedex, France

Key Words: Plasma; Surface modification; Hexatriacontane; Octadecyloctadecanoate; Model surface; XPS; Contact angle; FTIR

ABSTRACT

Surface functionalization by argon or oxygen RF plasmas (13.56 MHz) of polymer model compounds, namely hexatriacontane ($C_{36}H_{74}$) and octadecyloctadecanoate [OOD, $CH_3(CH_2)_{16}COO(CH_2)_{17}CH_3$], was studied using contact angle measurements, XPS, and FTIR-ATR. In order to gain a better insight into the plasma-surface interaction mechanisms, the effects of the main plasma parameters (treatment time, power, pressure, and flow rate) on functionalization were investigated. It was shown that an argon plasma is more efficient than an oxygen plasma and that the ester-containing model compound incorporated less oxygen than the paraffinic one. After 10 seconds of treatment, contact angle measurements showed that none of these plasma parameters affect in any way the properties of the uppermost surface layer; these depend only on the nature of the sample and on the gas used in the plasma. On

the other hand, ESCA, which allows a 70-Å in-depth probing, reveals the influence of the plasma parameters on both types of samples. IR, which probes to a much greater depth, evidences an evolution only for treated OOD samples. Interpretations are proposed for the effect of the plasma parameters on functionalization.

INTRODUCTION

Low temperature plasmas have been widely used to modify polymer surface properties like wettability and adhesion [1–7]. Surface modification is the result of the interactions between the polymer surface and the plasma active species such as ions, excited neutrals, and radicals as well as UV radiation. It is generally accepted that the first step consists of the formation of radicals on the surface layer by the elimination of hydrogen atoms. These radicals are able to react with oxygen atoms or molecules to produce functional groups such as alcohols, ketones, acids, and aldehydes. Their recombination also induces crosslinking or double-bond formation. Functionalization is always accompanied by surface degradation which results in a loss of weight and a modification of the surface topography. The relative importance of these two opposite processes depends on the nature of the polymer and also on the treatment conditions (time, applied power, gas flow rate, and gas pressure). The study of the influence of each parameter allows a better understanding of the interaction mechanisms and an optimization of the treatment process.

In order to predict the behavior of a polymer in cold plasmas, it is necessary to establish a relationship between the physical and chemical makeup of a polymer and its behavior in cold plasmas. Different polymers treated in the same plasma reactor under identical experimental conditions should be compared to reach this goal. The same polymer, however, can present different chemical compositions and structural morphologies at the surface depending on the preparation process (mold nature, cooling rate, etc.), and therefore its behavior will depend on it. Comparison of polymers that differ in their chemical compositions and which generally will have different crystalline area percentages is difficult because several parameters (chemical composition, crystallinity ratio) can interact.

In order to simplify this problem, we have chosen [8] to study the surfaces of crystalline molecules as models of polymers: hexatriacontane ($C_{36}H_{74}$), often used as a model of polyethylene in crystallization studies [9, 10], and octadecyloctadecanoate [$CH_3(CH_2)_{16}COO(CH_2)_{17}CH_3$, called OOD in the text]. This latter molecule is obtained by substitution of the central methylene of hexatriacontane by an ester group. $C_{36}H_{74}$ and OOD crystals are rhombic platelets, the acute angle of the lozenge being 72° [11, 12]. The chains are arranged perpendicularly to the crystal surface, the methyl groups being at the top and bottom. These molecules have the same crystalline structure, and the differences observed in their behavior can therefore be attributed to the presence of the ester function. As a second step that supports the choice of these model compounds, they have been compared to their corresponding polymers, i.e., high-density polyethylene and a polyester (polycaprolactone), and these results will be published in our next paper.

This article reports on the study of the functionalization of these model surfaces as a function of various operating conditions. Although plasma treatment is limited to the surface region, functionalization is not necessarily homogeneous within this layer [13–16]. Therefore, three techniques of increasing sampling depth were used to characterize the modifications induced by plasma treatment: contact angle measurements, XPS, and FTIR spectroscopy.

EXPERIMENTAL

Model Compounds

Hexatriacontane, purchased from Aldrich (purity 98%), was recrystallized from hexane.

OOD was synthesized by reacting octadecanol with octadecanoyl chloride at 90°C in chloroform in the presence of triethylamine as an HCl trap. The ester was purified by chromatography on a silica gel column and recrystallized from acetone.

The $C_{36}H_{74}$ and OOD films were prepared by melting under vacuum on aluminum plates set on a heating pad. The film thickness was about 2 μm. After preparation, the films were stored under argon.

Plasma Treatment

The plasma reactor was a stainless-steel cylindrical vessel, 15 cm in height and 23 cm in diameter. The power to sustain the plasma was supplied by a 13.56-MHz generator (ENI HF 300) which was capacitively coupled to the lid via an impedance matching network. The samples to be treated were placed on the grounded electrode which was kept at constant temperature by water circulating in its core. The chamber pressure was reduced to 10^{-2} torr (1 torr = 133.3 Pa). The gas was fed into the reactor through a mass flowmeter. The concentration of the species present in the plasma were followed as a function of time with a quadrupole mass spectrometer (SXP 300, VG Instruments, described elsewhere [17]) connected between the plasma reactor and the pump.

The experimental procedure was as follows. After setting up the sample ($C_{36}H_{74}$ or OOD film) in the chamber, the reactor pressure was reduced to 10^{-2} torr and the gas (argon or oxygen) was introduced at 100 cm^3(STP)/min for several minutes until the argon or oxygen concentration was at least 97% as measured by mass spectrometry. Typically, the initial gas composition for an argon plasma was 98% argon, 0.2% hydrogen, 0.7% water, 0.9% nitrogen, and 0.2% oxygen. For an oxygen plasma, it was 97% oxygen, 0.2% hydrogen, 1% water, 1.4% nitrogen, and 0.3% argon. Then the designated gas flow rate (ranging from 10 to 50 cm^3(STP)/min), power (20–100 W), and pressure (0.30–1.00 torr) were set and the plasma was started. The treatment lasted between 5 and 60 seconds as predetermined. After the end of the treatment, the sample was kept in the chamber for 10 more minutes while the same gas flow rate was applied. The reactor was then opened. The first sample of each new series of parameters was eliminated (see below). The following ones were stored under argon for a couple of hours. They were studied by contact angle measurements, XPS, or FTIR. Contact of the treated samples with air could not be avoided, but it was kept to a minimum.

Contact Angle Measurements

Static contact angles (sessile drop) were measured directly with the help of a Spindler and Hoyer device (Germany). Two sets of very pure test liquids, water and α-bromonaphtalene for hexatriacontane and water and methylene iodine for octadecyloctadecanoate, were used. The volume of the drop was always 2 μL. All measurements were performed a few minutes after treatment in a room with controlled temperature (23°C) and relative humidity (50%).

The best way to calculate surface energies from contact angle data is still controversial [18]. This problem will not be discussed here. We used the following classical approach. Surface energies were calculated from the contact angle data using the harmonic mean equation proposed by Wu [19]. The operative equation used was

$$\gamma_{LV}(1 + \cos\theta) = \frac{4\gamma_s^D\gamma_l^D}{\gamma_s^D + \gamma_l^D} + \frac{4\gamma_s^P\gamma_l^P}{\gamma_s^P + \gamma_l^P} \quad (1)$$

The components of the solid surface tension can be calculated provided the surface tension components of the test liquids are known and the contact angles of the two liquids are determined. This equation was reported to be the best approximation for organic liquids, polymers, water, etc. [20, 21].

XPS Analysis

XPS spectra were recorded on a VG ESCALAB MKII spectrometer using AlK_α excitation radiation from an x-ray source operated at 11 kV and 5 mA. The takeoff angle of the photoelectrons was 90°. Under our conditions, the mean free path of the electrons arising from the C_{1s} level is about 20 Å and the depth of analysis about 60 Å.

The constant analyzer energy mode was chosen with a pass energy of 50 eV. This high value was used in order to get a reasonable signal-to-noise ratio with a minimal irradiation time. Because charging effects were weak (2–4 eV) and almost constant from one sample to another, no flood gun was used. The base pressure in the analysis chamber was in the range 10^{-10} to 10^{-9} torr, but during a sample irradiation it rose to 10^{-8} torr. This was evidence of degradation reactions occurring under irradiation. It was further confirmed by the evolution of measured oxygen/carbon atomic ratios as a function of irradiation time. A hexatriacontane sample, treated for 20 seconds under an oxygen plasma (power 20 W and flow rate 10 cm^3/min), had an O/C atomic ratio of 0.110. After further x-ray irradiation (AlK_α, 11 kV, 10 mA) in the XPS chamber for 1 hour, the measured O/C atomic ratio had dropped to 0.061. The emission of the x-ray source was then lowered to 5 mA and the irradiation time was kept to a minimum. Typically, the carbon and oxygen peaks were recorded in about 5 minutes.

The peaks were plotted in such a way that the height of the maximum on the paper was always the same (see Fig. 3). This allows for an easier comparison of peak shapes. After recording the O and C peaks, the samples were systematically checked for contamination. It turned out that the main contaminant was silicon, so the range 0 to 200 eV (binding energy) was enough for this control. It was extremely difficult to get rid of this silicon contamination. Even when the samples were pre-

pared under strictly controlled conditions to avoid all contact with silicon, contamination sometimes reappeared in an apparent random manner. Contaminated samples were rejected.

In order to check for reproducibility, several experiments were performed. Four hexatriacontane samples were successively treated in an oxygen plasma (20 W, 10 cm^3/min, 10 seconds) and analyzed. The O/C atomic ratios were as follows: 0.086, 0.106, 0.110, and 0.110. This explains why the first treated sample was eliminated. The effect of the plasma treatment time was checked twice. Results were reproducible within an error range of 6%. Oxygen-to-carbon atomic ratios were obtained from area ratios of XPS peaks by using a relative sensitivity factor of 0.327. This factor was calculated in a classical way [22] detailed elsewhere [23].

FTIR Analysis

Fourier transform infrared spectra of the surface of the samples were obtained by the attenuated total reflection (ATR) technique. A Nicolet 60 SX FTIR instrument was used with an ATR 300 (Barnes, Spectra Tech, Inc.) multiple reflection unit. The internal reflection element was a germanium crystal (52 × 20 × 20 mm; entrance and exit angles 45°). It was carefully cleaned and dried under vacuum before use. Each spectrum resulted from the accumulation of 1000 scans at a resolution of 2 cm^{-1}. Subtraction of water and CO_2 absorbances were unnecessary in our working range (around 1700 and 700 cm^{-1}). A clamping force of 300 mN·m, applied by a torque wrench, was found to give good contact between the sample and the internal reflection element. Two thin (1 mm) rubber pads uniformly distributed the force provided by the pressure plates. With an incidence angle of 60°, the penetration depths of the IR beam into the samples were around 0.5 μm at 1700 cm^{-1} and 0.8 μm at 700 cm^{-1}. The bands of the carbonyl groups were normalized with respect to a band of the methylene group (CH_2 rocking) at 735–725 cm^{-1}. Normally, the stretching band at 1460 cm^{-1} should be used, but other bands overlap. This procedure compensated for variations in sample area and film-crystal contact.

RESULTS

The effect of the main treatment parameters on the functionalization of the two model surfaces ($C_{36}H_{74}$ and OOD) were studied. Results concerning the influence of treatment time, applied power, gas pressure, and gas flow rate will be successively presented. Two gases, oxygen and argon, were used throughout.

Influence of the Treatment Time

The variation of the surface tension (γ^T) of $C_{36}H_{74}$ and OOD as a function of treatment time is shown in Fig. 1(a). For the two samples treated with both gases, there is a marked increase in γ^T with treatment time until a plateau is reached between 10 and 20 seconds. The order of increasing surface tension is $OOD(O_2) < C_{36}H_{74}(O_2) < OOD(Ar) < C_{36}H_{74}(Ar)$. Argon is more efficient than oxygen, and

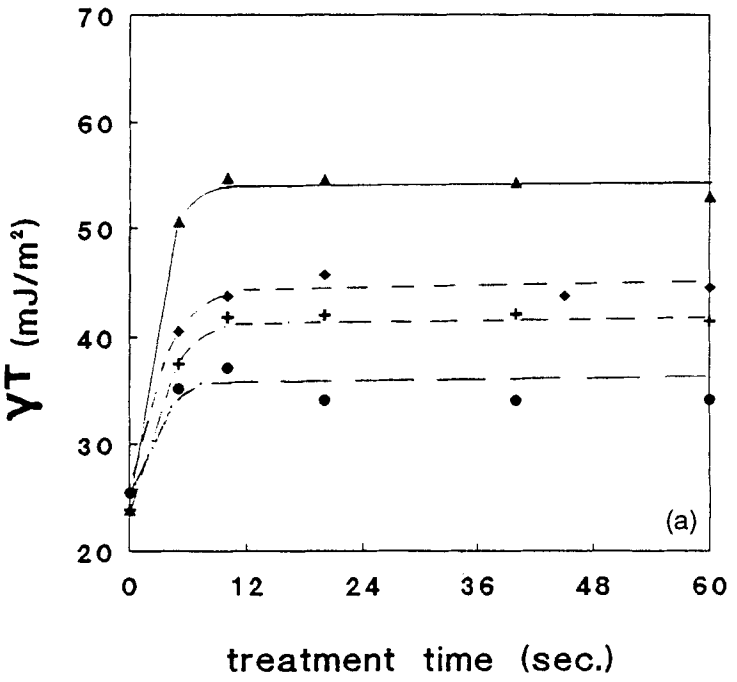

FIG. 1. Surface tension versus time of oxygen or argon plasma treatment for $C_{36}H_{74}$ and OOD. Other treatment conditions: 60 W, 40 cm_3(STP)/min, 0.3 torr. (a) Total surface tension (γ^T). (b) Polar component (γ^P). (c) Dispersive component (γ^D). (▲) $C_{36}H_{74}$ argon, (+) $C_{36}H_{74}$ oxygen, () OOD argon, (●) OOD oxygen.

the increase is more pronounced for $C_{36}H_{74}$ than for OOD. Both γ^P and γ^D contribute to the increase of γ^T (Figs. 1b and 1c).

Figure 2 shows the variation of the oxygen-to-carbon atomic ratio determined by XPS as a function of treatment time. Oxygen is incorporated into the surface layer of both samples treated with either gas. When the treatment time increases, O/C goes through a maximum and then decreases to a constant value. A sharp maximum is reached at 5 seconds for an oxygen plasma whereas it is broader and located around 20 seconds for an argon plasma. After an argon plasma treatment, almost the same amount of oxygen is incorporated into the surface layer of $C_{36}H_{74}$ and OOD. The initial difference in the O/C ratio (5%) due to the presence of oxygen in the ester compound is maintained whatever the treatment time. This is not true for oxygen plasmas. Far more oxygen is incorporated in $C_{36}H_{74}$ than in OOD. The increase of the oxygen-to-carbon ratio as determined by XPS is a direct measure of the incorporation of oxygen by the plasma treatment.

A qualitative analysis of the carbon peak shapes confirms the above results. Figure 3a shows the modifications of the C_{1s} peak as a function of treatment time in the case of OOD. It is clear that argon is more efficient than oxygen, and the shape of the curves in Fig. 2 is also confirmed by those in Fig. 3b (maximum at 20 seconds for Ar, at 5 seconds for O_2, etc.). Deconvolution of the C_{1s} peak in components corresponding to different oxygen functionalities was not performed because of the

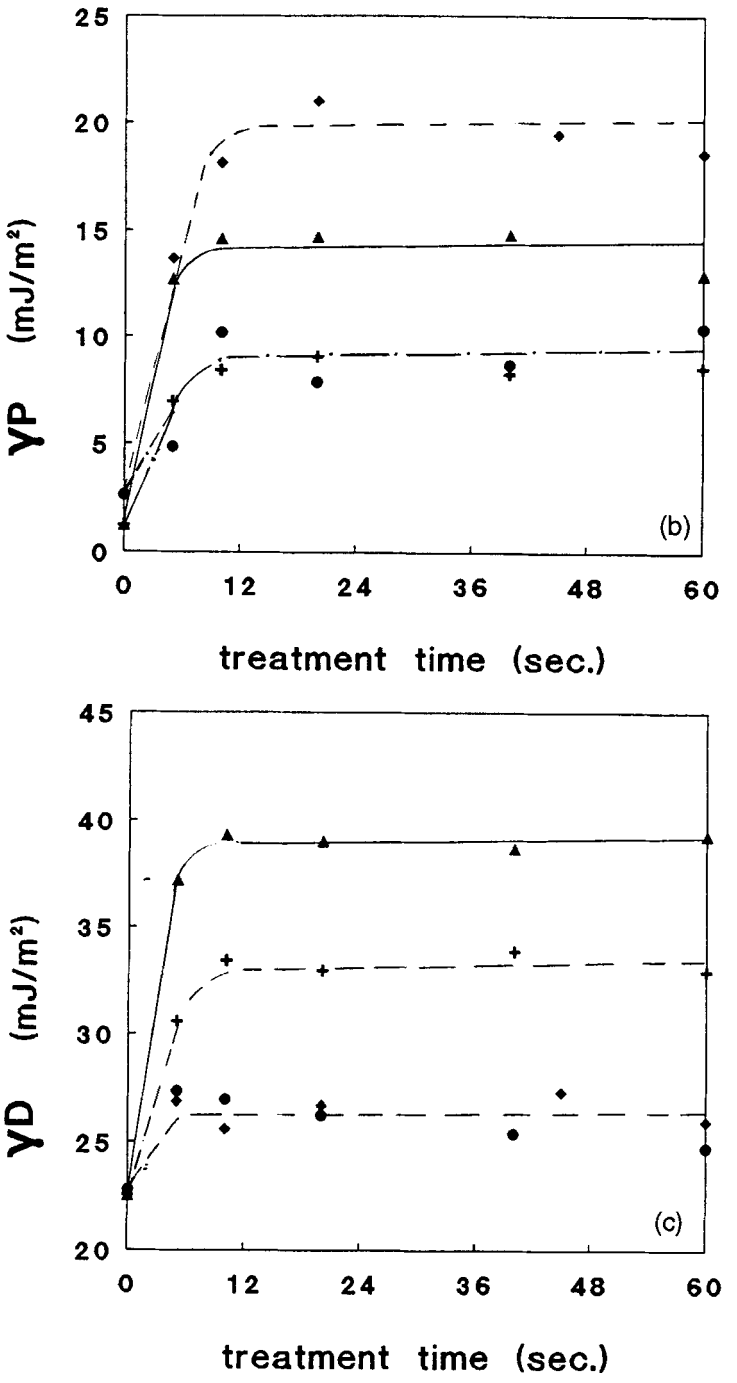

FIG. 1. Continued.

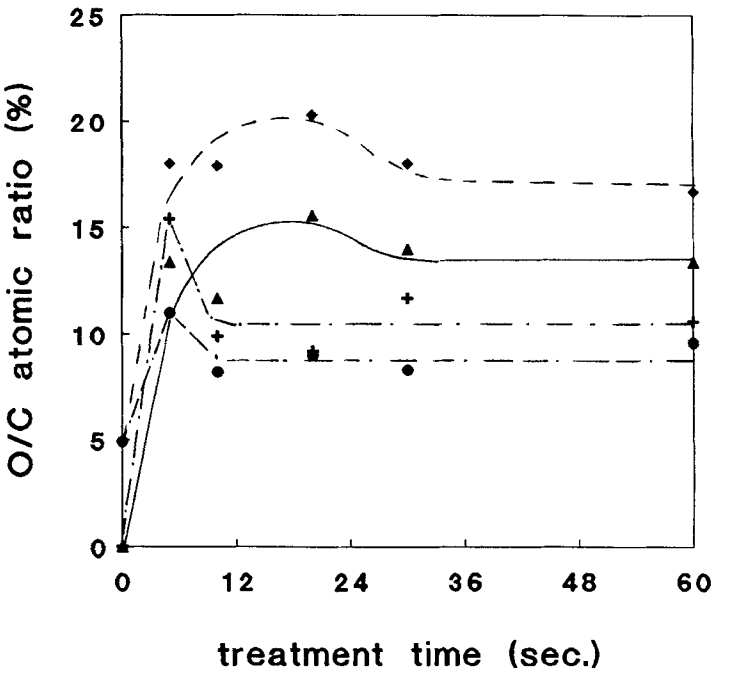

FIG. 2. Oxygen-to-carbon atomic ratio versus time of oxygen or argon plasma treatment for $C_{36}H_{74}$ and OOD. O/C ratios determined by XPS. Other treatment conditions: 60 W, 40 cm^3(STP)/min, 0.3 torr. ( ) $C_{36}H_{74}$ argon, (+) $C_{36}H_{74}$ oxygen, () OOD argon, (●) OOD oxygen.

poor resolution of the spectrometer used. The O_{1s} peak was always broad and symmetrical.

FTIR ATR analysis of the $C_{36}H_{74}$ samples revealed the appearance of absorption bands, especially around 1700 cm^{-1}. These bands were, however, very weak due to the superficiality of the plasma treatment and, possibly, to a bad film-crystal contact. They could not be used, even in a qualitative way. The carbonyl stretching region for the untreated and oxygen- or argon-treated OOD samples are presented in Figs. 4 and 5, respectively. The evolution of the absorption intensity in both figures can be compared if it is assumed that the depth probed on the nontreated samples is the same and that the absorption of the ester group is therefore equivalent before treatment. The oxygen plasma gives rise to a marked evolution of the IR absorption in the C=O stretching region as a function of treatment time. Between the untreated OOD and the sample treated for 60 seconds, the peak widens between 1780 and 1680 cm^{-1} and its area is multiplied by a factor of 6 after 60 seconds. This large absorption increases regularly with treatment time.

Several functions, such as aldehydes, ketones, acids conjugated or not with double bonds, and other carbonyl functions, can absorb in this wide band. Each of them will have its own extinction coefficient. To analyze the exact nature of the modification, determination of the extinction coefficient of a large number of reference molecules should be made. It should be noted that the C=O stretching band area is not a direct measure of the oxygen functionalization as was the O/C atomic

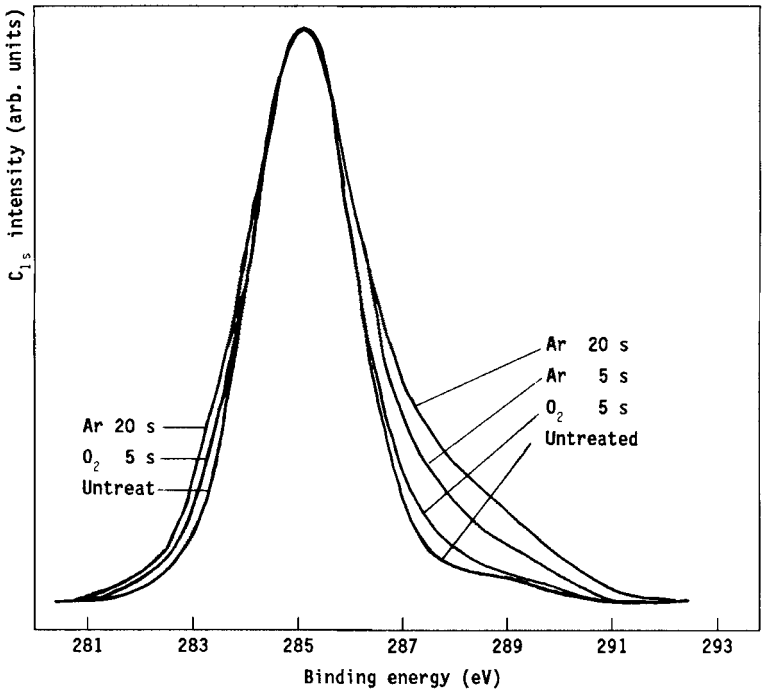

FIG. 3a. XPS C_{1s} peak shapes for OOD untreated or argon or oxygen plasma treated during various times. Other treatment conditions: 60 W, 40 cm^3(STP)/min, 0.3 torr.

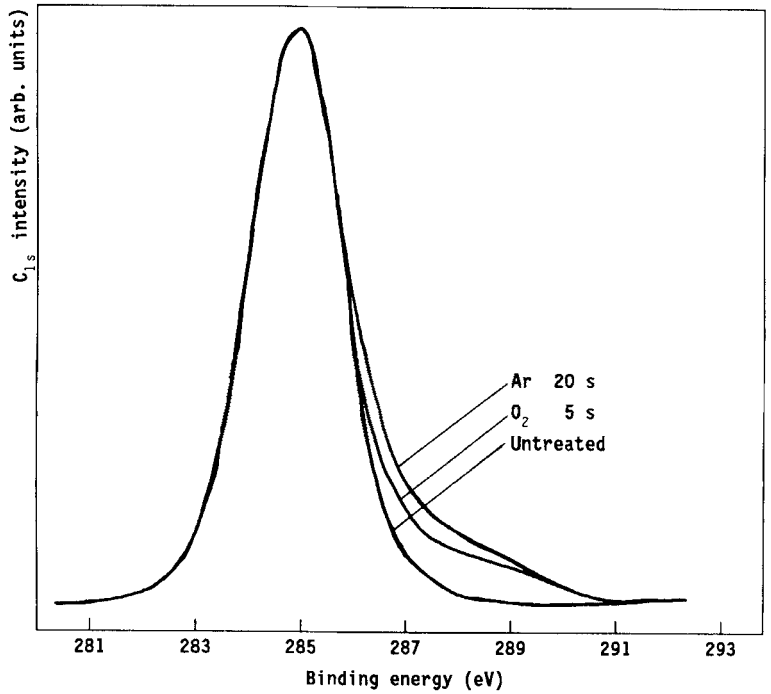

FIG. 3b. Comparison of XPS peak shapes for OOD for treatment times where the oxygen incorporation is the highest: 5 seconds in O_2 and 20 seconds in Ar.

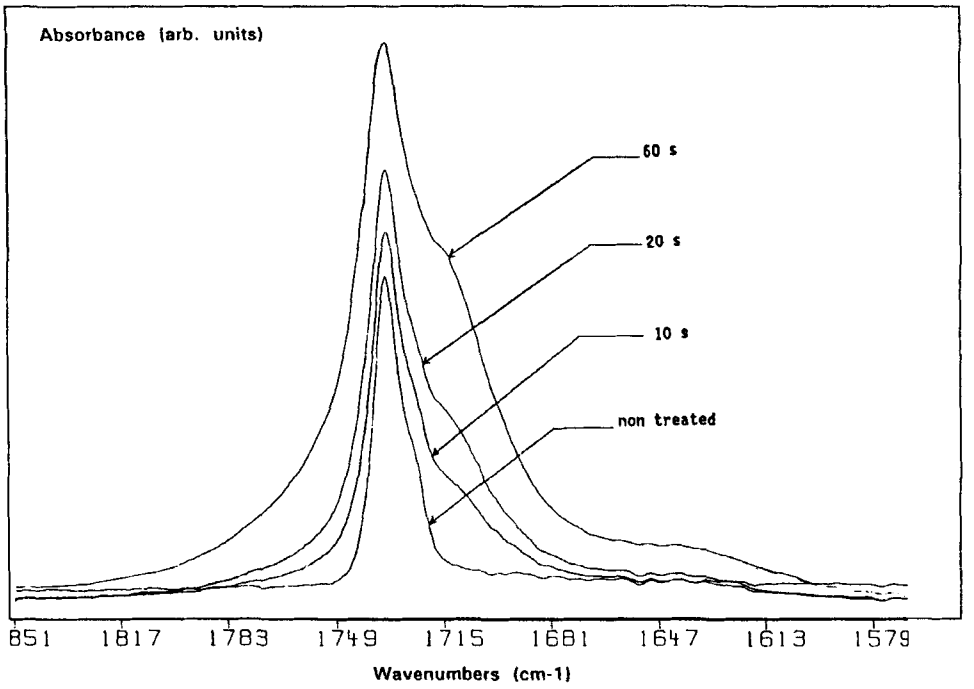

FIG. 4. Evolution of the FTIR ATR absorption bands in the carbonyl stretching region for OOD, untreated and oxygen plasma treated, during various times. Other treatment conditions: 60 W, 40 cm^3(STP)/min, 0.3 torr.

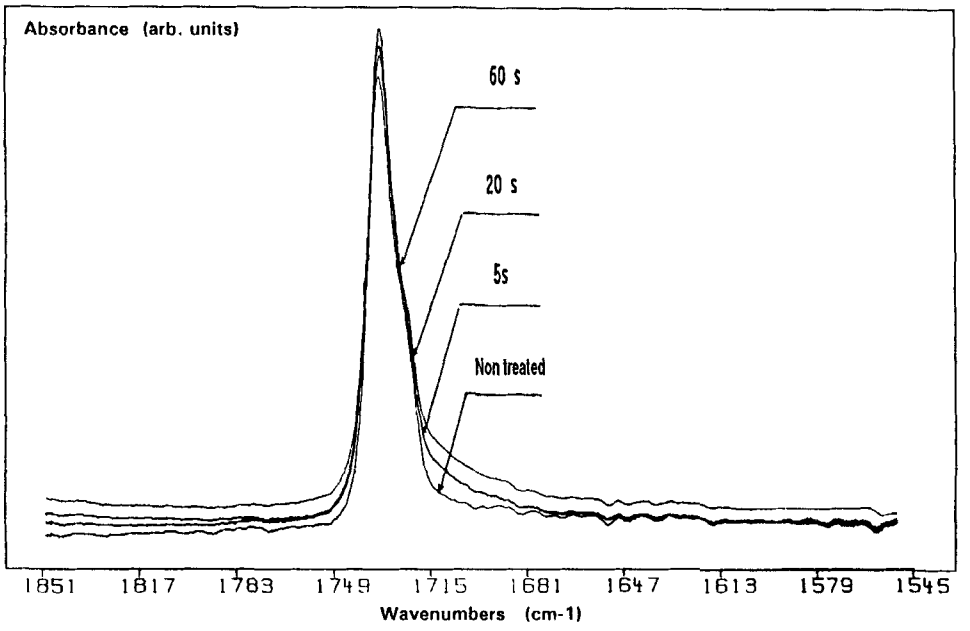

FIG. 5. FTIR ATR absorption bands in the carbonyl stretching region for OOD, untreated and argon plasma treated, during various times. Other treatment conditions: 60 W, 40 cm^3(STP)/min, 0.3 torr.

ratio derived from the XPS measurements. First, some hydroxyl groups may be created which would not be detected in the 1700 cm^{-1} region (analysis of the O—H or C—O absorption bands was too difficult). Second, modifications of the environment of the carbonyl group can provoke alterations of its molar adsorption coefficient (ϵ). For example, if the ester is modified into a ketone, ϵ is reduced by a factor of 1.44 [24]. Alteration of the carbonyl absorption band after oxygen plasma treatment of OOD demonstrates modification of the surface, and this appears to be quite high as compared to that observed for $C_{36}H_{74}$.

Figure 5 is the equivalent of Fig. 4 except for an argon plasma treatment of OOD. The difference is striking. In this case there is only the appearance of a weak absorption around 1720–1680 cm^{-1}.

Influence of the Treatment Power

Between 20 and 100 W (other parameters of the plasma treatment: 40 cm^3 (STP)/min, 0.3 torr, and 60 seconds), there is no significant effect of the power on the surface tension. The data are very similar to those in Fig. 1(a).

The incorporation of oxygen into the surface region as a function of treatment power is shown in Fig. 6. It is measured by the oxygen over carbon atomic ratio as determined by XPS. The power has no effect for oxygen plasmas, but the oxygen functionalization increases for argon plasma. In that case a plateau is reached at 60 W for OOD and 80 W for $C_{36}H_{74}$.

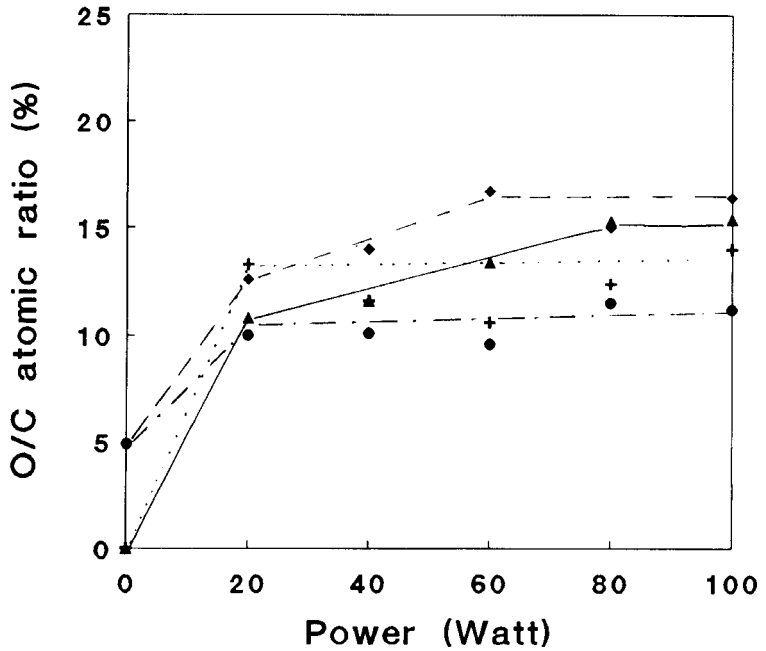

FIG. 6. Oxygen-to-carbon atomic ratio (determined by XPS) versus power of oxygen or argon plasma treatment for $C_{36}H_{74}$ and OOD. Other treatment conditions: 40 cm^3(STP)/min, 0.3 torr, 60 seconds. (▲) $C_{36}H_{74}$ argon, (+) $C_{36}H_{74}$ oxygen, () OOD argon, (●) OOD oxygen.

For OOD treated by an oxygen plasma, the area of the FTIR ATR absorption band in the carbonyl stretching region (Fig. 7) increases when the power is increased from 20 to 60 W and then decreases to the 40 W level for 80 and 100 W. As in the case of the time influence (Fig. 5), there is no detectable power effect when OOD is treated by an argon plasma. For $C_{36}H_{74}$, no relevant information could be obtained from the FTIR ATR spectra due to the weakness of the bands which appeared after treatment.

Influence of the Gas Pressure

The effect of increasing gas pressure (from 0.3 to 1 torr) is shown in Figs. 8 (O/C atomic ratio) and 9 (carbonyl stretching band). The other processing parameters were kept at the following constant values: 60 W, 40 cm^3(STP)/min, 60 seconds. The effect of gas pressure is negligible on the surface tension; again, the data are very similar to those in Fig. 1(a). The O/C ratio is not significantly affected for argon plasmas (Fig. 8); for oxygen plasmas there is a maximum at 0.65 torr. The effect on the IR peaks is not very clear (Fig. 9, OOD, oxygen plasma). The most pronounced effect is at 0.3 torr, the least at 0.5 torr, and intermediate effects at in-between pressures (0.65, 0.8 and 1.0 torr).

Influence of the Gas Flow

The influence of gas flow during plasma treatment is presented in Fig. 10. In this study the power was kept at 60 W, the pressure at 0.3 torr, and the time at 60 seconds. The flow rate does not significantly affect the surface tension (data like

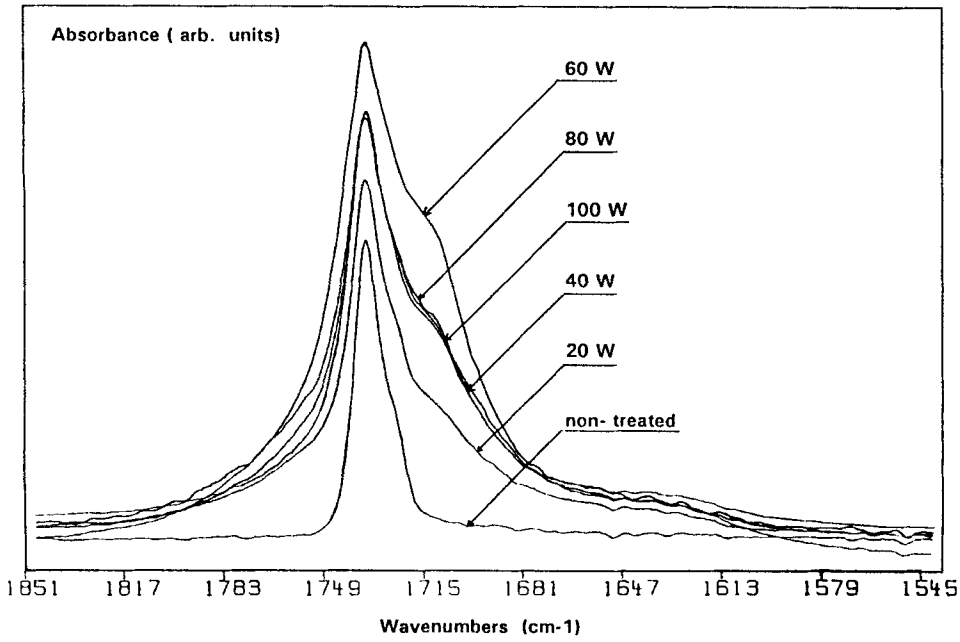

FIG. 7. FTIR ATR absorption bands in the carbonyl stretching region for OOD, untreated and oxygen plasma treated, with various applied powers. Other treatment conditions: 40 cm^3(STP)/min, 0.3 torr, 60 seconds.

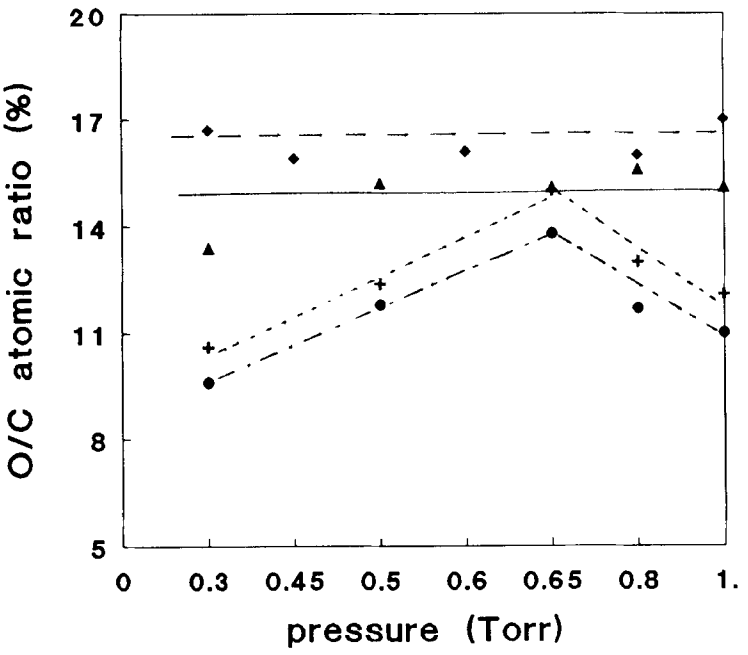

FIG. 8. Oxygen-to-carbon atomic ratio (determined by XPS) versus gas pressure of oxygen or argon plasma treatment for $C_{36}H_{74}$ and OOD. Other treatment conditions: 60 W, 40 cm^3(STP)/min, 60 seconds. (▲) $C_{36}H_{74}$ argon, (+) $C_{36}H_{74}$ oxygen, (♦) OOD argon, (●) OOD oxygen.

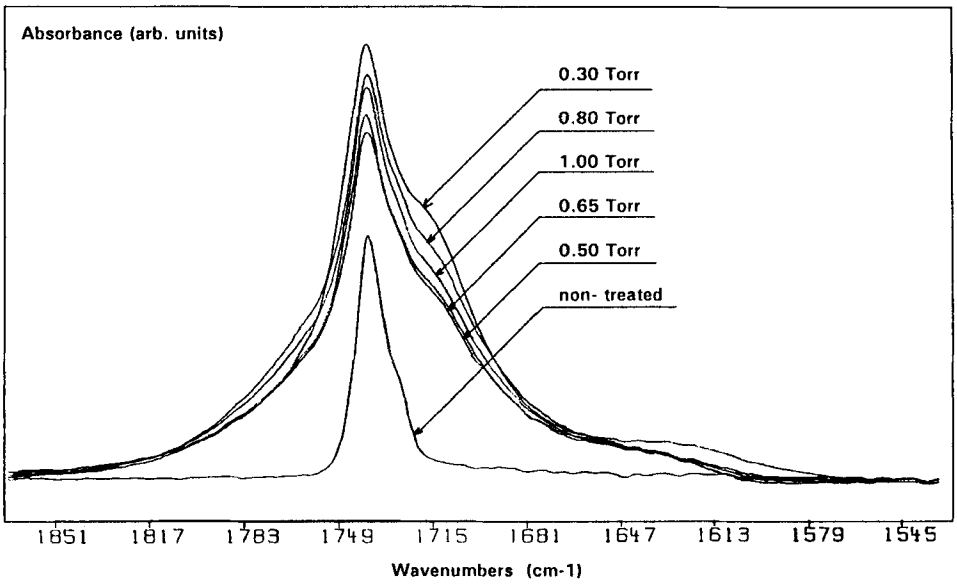

FIG. 9. FTIR ATR absorption bands in the carbonyl stretching region for OOD, untreated and oxygen plasma treated with various gas pressures. Other treatment conditions: 60 W, 40 cm^3(STP)/min, 60 seconds.

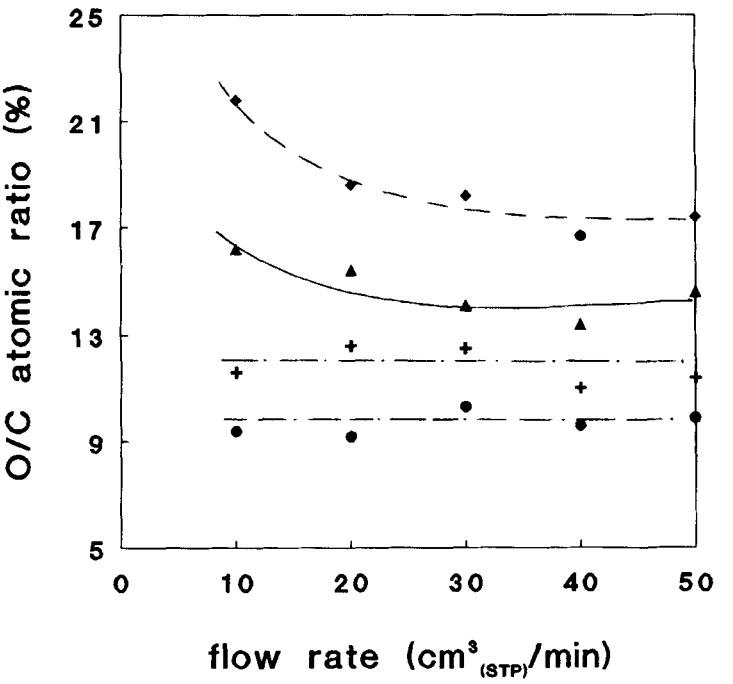

FIG. 10. Oxygen-to-carbon atomic ratio (determined by XPS) versus gas flow of oxygen or argon plasma treatment for $C_{36}H_{74}$ and OOD. Other treatment conditions: 60 W, 0.3 torr, 60 seconds. (▲) $C_{36}H_{74}$ argon, (+) $C_{36}H_{74}$ oxygen, (♦) OOD argon, (●) OOD oxygen.

those on Fig. 1a) and the O/C ratio for oxygen plasmas (Fig. 10). The O/C ratio decreases, however, with an increasing flow rate for argon plasmas (Fig. 10).

DISCUSSION

The effect of the main plasma parameters (time, power, pressure, and gas flow) on surface modification is variable and depends on the thickness of the layer under consideration. When the uppermost layer was studied by contact angle measurements (Fig. 1), three important results emerged which will be discussed below: argon plasma is more efficient than oxygen plasma in terms of a surface energy increase; $C_{36}H_{74}$ contains more functional groups than does OOD; and, for a given sample-gas combination, none of the plasma parameters affects chemical modification, i.e., within experimental error, the surface energy data are identical.

It is surprising that more oxygen functions are incorporated into the surface by an argon plasma than by an oxygen plasma. The modification processes are very different in the two plasmas. With an Ar plasma, the first step is the formation of radicals at the surface by interaction with the active species of the plasma [25–29]. These radicals can react with each other to cause crosslinking or branching. They can also produce unsaturations by the reaction [30]:

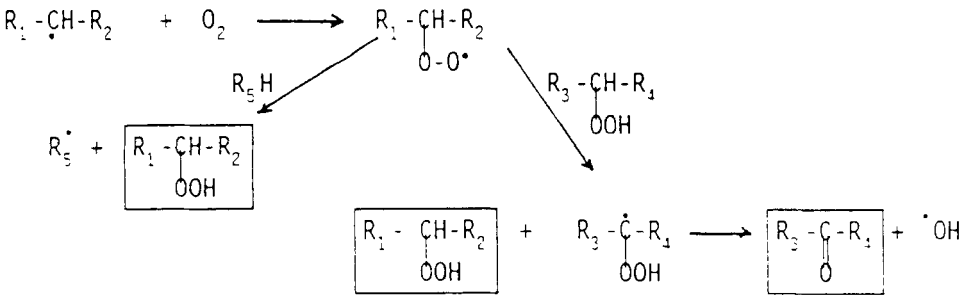

SCHEME 1.

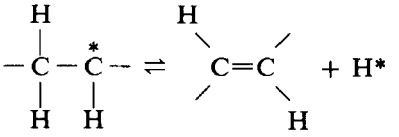

The hydrogen atom can react with another hydrogen atom to give the main degradation product which is H_2 [17]. In our opinion, degradation reactions are only those reactions which induce a loss of weight of the sample by ejection of matter. At the end of the plasma treatment, some radicals remain trapped in the sample and react with oxygen in air when the plasma chamber is opened. When alkyl radicals react with molecular oxygen, the set of principal reactions shown in Scheme 1 has been proposed [31, 34, 35].

Ketones and hydroperoxides can react with each other to give essentially alcohols, ketones and ethers according to the different reactions described by Gugumus [31]. For OOD, it is possible that carbonyl radicals are also trapped. In this case, the formation of acids according to Scheme 2 cannot be excluded.

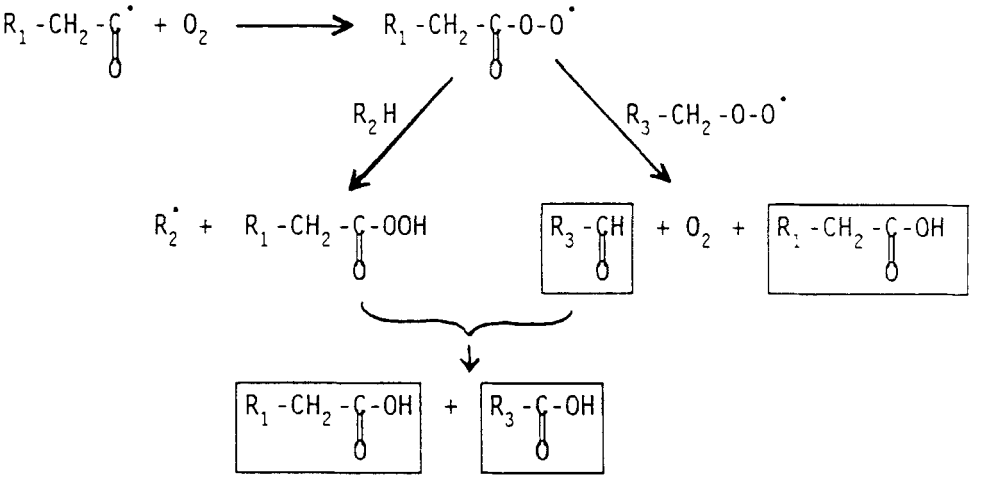

SCHEME 2.

If the modification observed in the case of an argon plasma results only from the reaction between trapped radicals and oxygen in the air, then ketones, alcohols, and ethers should be mainly found on the hexatriacontane while the acid concentration should be higher on OOD. It is also possible that oxygen traces (less than 0.2%) remaining in the chamber contributed to the functionalization as reported by Clark et al. [15], who showed that oxygen incorporation was higher in a helium–oxygen (95–5%) mixture than in a pure oxygen plasma. These functions, which may be different in number and nature on $C_{36}H_{74}$ and OOD, may explain why the surface energy of OOD is smaller than that of $C_{36}H_{74}$, although oxygen incorporation is equivalent for both samples. This hypothesis should be supported by the determination of radical and acid function concentrations.

With an oxygen plasma, the production of radicals in the sample also occurs during the first step. However, the evolution of these radicals is different because they are able to react not only with molecular oxygen but also very quickly with atomic oxygen. This can give rise to an extremely complex set of reactions in which (as demonstrated by gravimetry, mass spectrometry and optical emission spectrometry [17]) degradation is very important; it is 15 times faster in oxygen than in argon and is close to 26 $\mu g/cm^2 \cdot min$. The functional groups which form in an oxygen plasma may subsequently react with other plasma active species, in particular, photons. Photons can activate the hydroperoxide, ketone, and aldehyde functions formed (Scheme 1) and induce numerous other reactions leading to cleavage of an α-ketone chain:

$$R-\underset{\underset{O}{\|}}{C}-R' + h\nu \rightarrow R-\underset{\underset{O}{\|}}{C}^{\cdot} + R^{\cdot}$$

and the formation of acid functions according to Scheme 2.

A small number of radicals may also remain trapped at the end of treatment and react with oxygen in the air. Therefore, due to the importance of degradation reactions in an oxygen plasma, the incorporation of oxygen functions is less marked than in an argon plasma. Similar results were obtained by other authors, such as Blythe et al. [32] who observed a higher O/C ratio for Ar than for air and Chen [27] who recently showed that the efficiency of a plasma to create radicals decreases in the order $CO > Ar > N_2 > O_2$.

Another phenomenon could also contribute to the difference between argon and oxygen plasmas. Plasma-modified surfaces may reorganize to become thermodynamically more stable by migration away from the surface of the highly polar low molecular weight species. The oxygen plasma, because of higher degradation, produces a higher proportion of low molecular weight, mobile species than the argon plasma which tends to lock the surface through crosslinking [14]. By the time the measurements are made, some of the oxygen-containing mobile species produced in the oxygen plasma may have migrated toward the bulk. This migration would be less likely at the surface of the argon-treated sample because of a lack of mobility. However, this interpretation is difficult to verify.

In an oxygen plasma, the OOD is less functionalized than $C_{36}H_{74}$ and more degraded due to the presence of the ester function [17]. Moreover, in an Ar plasma, oxygen can be extracted from the OOD sample and will then participate in further degradation reactions. Most likely it is because of faster degradation reactions that

OOD is less functionalized than $C_{36}H_{74}$. This has been confirmed by other studies. Yasuda et al. [33] showed that oxygen incorporation is less pronounced in polymers which already contain some oxygen (PET, POM, PA6, cellulose acetate) as compared to polymers without oxygen (PE, PS, PTFE).

After 10 seconds of treatment, the composition and topography of the uppermost surface layer depends only on the sample–gas couple. In an argon plasma, an equilibrium is reached between the processes which create radicals and the reactions which make them disappear. In the O_2 plasma, a fast equilibrium is reached between oxygen incorporation and ejection of oxygen-containing species. Fast equilibrium is no longer observed when thicker surface layers are considered. When layers in the range below 70 Å (XPS sampling depth) are studied, the effects of the plasma parameters become significant. These effects will be discussed in the following sections.

Influence of the Time of Treatment

In the layer probed by ESCA, the evolution versus time of the O/C ratio is the same for hexatriacontane and OOD.

In the case of an oxygen plasma, incorporation of oxygen results from reactions taking place in the plasma, and the decrease observed after a 5-second treatment should be due to the attack of the oxygenated functions just formed by the active species of the plasma. The plateau which is then reached corresponds to an equilibrium between the formation and the degradation of the functions. This result agrees with that reported by Clark [13, 14] for polyethylene treated in an oxygen plasma.

In an argon plasma, reactions between trapped radicals and air are claimed [25–28] to be responsible for oxygen incorporation. During the treatment, a radical formed by the breaking of a bond can be consumed by recombination or disproportionation as long as its mobility is sufficient. A radical can migrate along the chain by intermolecular and intramolecular chain transfer, but it is not consumed until it encounters another radical. The mobility of a radical is reduced either because of the crystalline moieties or because of the crosslinking taking place which increases with treatment time. Both effects work toward radical trapping. According to the evolution data shown in Fig. 2, the trapped radical concentration reaches a maximum after 20 seconds in the layer probed by ESCA. Since the degradation rate is constant over time [17], the subsequent decrease of oxygen incorporation between 20 and 30 seconds can be due to the formation of a more compact network generated by bond breaking. Afterwards, an equilibrium between radical trapping and degradation should be reached. This decrease can also be explained by the fact that the hydroperoxides formed after treatment are not very stable. In addition, although samples are stored at room temperature, as the concentration of oxygenated functionalities increases, their decomposition or reaction with neighboring ketones cannot be excluded.

When a thicker surface layer is studied (ATR sampling depth, around 0.5 μm) (Figs. 4 and 5), the difference due to the two gases becomes striking in the case of OOD. For an argon plasma, there is a very slight change in the shape of the IR absorption band around 1700 cm^{-1} as a function of treatment time (Fig. 5). A weak absorption peak appears around 1720–1690 cm^{-1}, characteristic of acids,

α,β-unsaturated acids, and aldehydes. Nevertheless, its intensity is negligible as compared to the evolution observed in an oxygen plasma where the global absorption intensity in the range 1780–1680 cm^{-1} is six times greater. This can be due to a modified surface layer which is very thin or to the formation of functions which do not absorb in this wavelength range. When oxygen is used in the plasma, there is a marked effect of time (Fig. 4) which indicates that the evolution detected in the depth probed lasts longer than in that detected by ESCA. The equilibrium between the formation and the degradation of the chemical functions seems to be reached faster in the layer probed by ESCA than in the depth seen by IR in the case of OOD. Nguyen et al. [37] also found an increase of carbonyl absorption for 10 minutes in the low-density polyethylene treated in an oxygen plasma, but in our work with $C_{36}H_{74}$, the absorption of carbonyl functions was too low for its evolution to be followed, at least for the first minute.

This can be due to the diffusion of atomic oxygen toward the bulk of the sample during plasma treatment. The diffusion process is time-dependent, but an explanation for the lack of diffusion of oxygen-active plasma in $C_{36}H_{74}$ cannot be given.

Influence of the Power

The treatment time was maintained at 60 seconds, which is sufficient to reach a steady amount of oxygen incorporation in the 70-Å thick layer (Fig. 2). An increase of power of the plasma increases the number of active species and therefore induces a rise of the rates of the reactions responsible for chemical modification: functionalization, degradation, and crosslinking.

In the case of an oxygen plasma, the emission of atomic oxygen species increases as $P^{2.3}$, where P is the power [17]. Assuming that the curve shapes shown in Fig. 2 do not depend qualitatively on power, the slopes of the increase and the location of the maxima are probably power-dependent [26]. However, in the power range studied, the equilibrium between the formation of functional groups and their degradation appears to be independent of power, at least in terms of oxygen incorporation. This does not mean that the nature and the number of each function found after treatment are exactly the same over the entire range.

On the other hand, for an argon plasma, although the evolution is weak, the level of the plateau increases with the power (Fig. 6). The Ar-excited species emission increases as $P^{0.42}$, more slowly than the atomic oxygen emission in an oxygen plasma. Therefore, it is possible that the level of radicals trapped after 1 minute can increase in the power range studied and will reach a constant value beyond 1 minute.

At higher thicknesses (Fig. 7), the power rise increases with the concentration of atomic oxygen in the plasma, which in turn increases the diffusion of atomic oxygen toward the bulk. Thus, functionalization is increased in the surface layer sampled by ATR. However, the degradation rate (R_D) increases linearly with power (P_W) according to

$$R_D = 0.27P_W + b_c$$

Above 60 W, the competition between degradation and oxygen incorporation induces a decrease in the global functionalization of the layer analyzed by IR. This

evolution agrees well with the results of Nguyen et al. [37] and Urban and Stewart [38] in their FTIR-ATR studies of PE treatment by an O_2 plasma.

Influence of the Pressure

The number of species in the plasma increases with pressure. When the power remains constant, these species share a constant energy, and thus the concentration of active species decreases. Reactivity threshold effects are likely to appear. Figure 8 shows the O/C atomic ratio in the 70-Å thick layer. For argon, despite the increase in the total number of species, the proportion able to create radicals seems to remain constant. For oxygen, functionalization starts to increase, reaches a maximum at 0.65 torr, and then, as too many species share a constant amount of available energy, the number of species able to create radicals decreases. The difference between $C_{36}H_{74}$ and OOD is apparent at greater depths. In the case of OOD (Fig. 9), a complex pattern is observed. When the pressure increases, diffusion is expected to increase. At the same time, the distribution of the various kinds of activated species changes with pressure. The rate of diffusion is probably different for the different kinds of oxygen species. Furthermore, the reactivity of the diffusing species tends to decrease with increasing pressure. The balance between these opposite effects evolves in a complicated way with pressure. This may explain the peculiar pressure dependence observed in Fig. 9. The influence of pressure on evolution in the layer probed by IR is small compared to that of power or time. A regular decrease of the $-C=O$ absorption intensity was observed by Nguyen et al. [37] for a longer reaction time (10 minutes). The reactor used was an electrodeless discharge, and the results cannot be compared directly. Nevertheless, the decrease observed by these authors agrees better with the ESCA results where the maximum will most likely depend on the mean energy input per gas molecule, which differs in the two reactors.

Influence of the Flow Rate

The effect of an increase in the flow rate is a decrease in the residence time of the species in the plasma and at the surface of the sample. This does not affect the reactions at the uppermost surface, as mentioned above. To interact with and modify the inside of the sample, a species has to diffuse. Before diffusing, a species has to adsorb in some fashion at the surface. This adsorption process may be affected by changes in the flow rate. As the flow rate increases, adsorption may become hindered to a certain extent, and this could explain the diminution of functionalization in the 70-Å layer for an argon plasma (Fig. 10).

CONCLUSION

This work on model compounds deals with the influence of the introduction of an ester group on the functionalization of a hydrocarbonated surface by cold plasmas. The main results of this work can be summarized as follows.

An argon plasma is more efficient than an oxygen plasma for the introduction of oxygen functionalities at the surface of our model compounds. The difference in the oxygen incorporation mechanisms accounts for this apparent paradox.

A model compound containing an ester group (OOD) is less easily functionalized than a paraffinic one ($C_{36}H_{74}$). This is due to the fact that an oxygen-bearing site has a greater probability of undergoing a set of reactions leading eventually to extractable degradation products.

Functionalization varies very much with depth. After 10 seconds of treatment, the uppermost surface layer reaches a state of saturation with oxygen totally independent of the plasma parameters as observed by contact angle measurements. By using ESCA, the effect of the parameters becomes observable in the first 70 Å thick layer. When IR is used, a greater depth can be investigated but we observed a modification only in the case of an OOD sample treated with an oxygen plasma; this can be due to the diffusion of atomic oxygen inside the sample during treatment.

Analysis of the effect of the plasma parameters allows good insight into the plasma-surface interaction mechanisms. We have proposed several interpretations, but they remain speculative to a considerable extent. This is due to a lack of precise information on the characteristics of the plasma and also on the modified surface.

This work will be followed by a study of the corresponding polymers which will take into account their crystallinity. We plan to compare high density polyethylene to $C_{36}H_{74}$ and a polyester, polycaprolactone $[-(CH_2)_5COO-]_n$, to OOD. This comparison should allow for a further step in our understanding of plasma-surface interactions.

REFERENCES

[1] M. Strobel, S. Corn, C. S. Lyon, and G. A. Korba, *J. Polym. Sci., Polym. Chem. Ed., 23*, 1125 (1985).
[2] R. Foerch, N. S. McIntyre, and D. H. Hunter, *Ibid., 28*, 803 (1990).
[3] Y. L. Hsieh, D. A. Timm, and M. P. Wu, *J. Appl. Polym. Sci., 38*, 1719 (1989).
[4] D. Briggs, D. G. Rance, C. R. Kendall, and A. R. Blythe, *Polymer, 21*, 895 (1980).
[5] T. J. Hook, J. A. Gardella Jr., and L. Salvati Jr., *J. Mater. Res., 2*, 117 (1987).
[6] D. T. Clark and R. Wilson, *J. Polym. Sci., Polym. Chem. Ed., 21*, 837 (1983).
[7] E. Occhiello, M. Morra, G. Morini, F. Garbassi, and P. Humphrey, *J. Appl. Polym. Sci., 42*, 551 (1991).
[8] M. K. Shi, Y. Holl, Y. Guilbert, and F. Clouet, *Makromol. Chem., Rapid Commun., 12*, 277 (1991).
[9] D. L. Dorset, *J. Macromol. Sci.—Phys., B25*, 1 (1986).
[10] A. Kawaguchi, M. Ohara, and K. Kobayashi, *Ibid., B16*, 193 (1979).
[11] R. Boistelle, B. Simon, and G. Pepe, *Acta Cryst., B32*, 1240 (1976).
[12] F. Zemlin and D. L. Dorset, *Ultramicroscopy, 21*, 263 (1987).
[13] D. T. Clark, W. J. Feast, W. K. R. Musgrave, and I. Ritchie, *J. Polym. Sci., Polym. Chem. Ed., 13*, 857 (1975); *17*, 957 (1979).

[14] D. T. Clark and A. Dilks, *Ibid., 15*, 2321 (1977).
[15] D. T. Clark and A. Dilks, *Ibid., 17*, 957 (1979).
[16] M. Anand, R. E. Cohen, and R. F. Baddour, *Polymer, 22*, 361 (1981).
[17] F. Clouet and M. K. Shi, *J. Appl. Polym. Sci.*, In Press.
[18] M. Raetzsch, H. J. Jacobasch, and K. H. Freitag, *Adv. Colloid Interface Sci., 31*, 225 (1990).
[19] S. Wu, *J. Polym. Sci., Polym. Symp., C34*, 19 (1971).
[20] S. Wu, *Polymer Interface and Adhesion*, Dekker, New York, 1982.
[21] J. D. Andrade, S. M. Ma, R. N. King, and D. E. Gregonis, *J. Colloid Interface Sci., 72*, 488 (1979).
[22] J. D. Andrade, *Surface and Interfacial Aspects of Biomedical Polymers*, Vol. 1, Plenum Press, New York, 1985, p. 105.
[23] C. L. Zhao, F. Dobler, T. Pith, Y. Holl, and M. Lambla, *J. Colloid Interface Sci., 128*, 437 (1989).
[24] Z. Fodor, M. Irving, F. Tudos, and T. Kelen, *J. Polym. Sci., Polym. Chem. Ed., 22*, 2539 (1984).
[25] R. G. Nuzzo and G. Smolinsky, *Macromolecules, 17*, 1013 (1984).
[26] M. Suzuki, A. Kishida, H. Iwata, and Y. Ikada, *Ibid., 19*, 1804 (1986).
[27] J. R. Chen, *J. Appl. Polym. Sci., 42*, 2035 (1991).
[28] H. S. Munro and C. Till, *J. Polym. Sci., Polym. Chem. Ed., 24*, 279 (1986).
[29] N. Norosoff, B. Crist, M. Burmgarner, T. Hsu, and H. Yasuda, *J. Macromol. Sci.-Chem., A10*, 451 (1976).
[30] H. Schonhorn and R. Hansen, *J. Appl. Polym. Sci., 11*, 1461 (1967).
[31] F. Gugumus, *Angew. Makromol. Chem., 182*, 111 (1990).
[32] A. R. Blythe, D. Briggs, C. R. Kendall, D. G. Rance, and V. J. I. Zichy, *Polymer 19*, 1273 (1978).
[33] H. Yasuda, H. C. Marsh, E. S. Brandt, and C. N. Reilley, *J. Polym. Sci., Polym. Chem. Ed., 15*, 991 (1977).
[34] B. Ranby and J. F. Rabek, in *Photodegradation, Photooxidation and Photostabilization of Polymers*, Wiley, New York, 1975.
[35] J. Petruf and J. Marchal, *Radiat. Phys. Chem., 16*, 27 (1980).
[36] D. W. Fakes, J. M. Newton, J. F. Watts, and M. J. Edgell, *Surf. Interface Anal., 10*, 416 (1987).
[37] L. T. Nguyen, N. H. Sung, and N. P. Suh, *J. Polym. Sci., Polym. Lett. Ed., 18*, 541 (1980).
[38] M. W. Urban and M. T. Stewart, *J. Appl. Polym. Sci., 39*, 265 (1990).

Received February 6, 1992
Revision received August 3, 1992